Fermi National Accelerator Laboratory

FERMILAB-Conf-82/50-EXP
7550.537

PRODUCTION OF MUON PAIRS WITH MASSES GREATER THAN 4 GeV/c^2
IN $\bar{p}N$ AND π^-N INTERACTIONS AT 125 GeV/c*

E. Anassontzis, S. Katsanevas, P. Kostarakis, C. Kourkoumelis, A. Markou,
L. K. Resvanis, and G. Voulgaris
University of Athens, Athens, Greece

and

M. Binkley, B. Cox, J. Enagonio, C. Hojvat, D. Judd, R. D. Kephart,
P. K. Malhotra, P. O. Mazur, C. T. Murphy, F. Turkot, R. L. Wagner,
D. Wagoner, and W. Yang
Fermi National Accelerator Laboratory, Batavia, Illinois 60510 USA

and

H. Areti, S. Conetti, P. Lebrun, D. Ryan, T. Ryan, W. Schappert,
and D. Stairs
McGill University, Montreal, Canada

and

C. Akerlof, P. Kraushaar, D. Nitz, and R. Thun
University of Michigan, Ann Arbor, Michigan 48104 USA

and

He Mao and Zhang Nai-jian
Shandong University, Jinan, Shandong, Peoples Republic of China

July 1982

ABSTRACT

We have measured the high mass ($M > 4$ GeV/c^2) dimuons produced in anti-proton-nucleon and pi minus-nucleon interactions. Preliminary differential cross sections are presented as a function of pair mass, x_F, p_T, and $\sqrt{\tau}$. Comparisons of these cross sections with the predictions of the Drell-Yan model are discussed and preliminary values for the K factor for the $\bar{p}$ and π^- induced reactions are reported.

---

*Presented at the XXI International Conference on High Energy Physics, Paris, France, July 26-31, 1982.

Operated by Universities Research Association Inc. under contract with the United States Department of Energy

The study of the production of the high mass dilepton continuum by antiproton and by pi minus allows tests of the constituent picture of hadronic production of dileptons. Because of the greater knowledge of the valence quark structure functions of the nucleons and the dominance of the valence quark-antiquark annihilation in $\bar{p}N$ interactions, the antiproton reaction is a particularly valuable test of the current models of dilepton production. In this paper we report on the simultaneous measurement of dimuon production in both antiproton-nucleon and pi minus-nucleon interactions at 125 GeV/c.

This measurement was performed in the High Intensity Laboratory in the Proton Area at Fermilab with the large aperture forward spectrometer shown in Fig. 1. A unique 125 GeV/c enriched antiproton beam[1] of intensity 2×10^6 $\bar{p}$ and 8×10^6 π^- per 5×10^{12} incident 400 GeV/c protons was used in this experiment. A neutral beam was formed by sweeping all charged particles produced in the primary production target and collecting the antiprotons from the $\bar{p}\pi^+$ decays of the $\bar{\Lambda}^0$ component of this beam. The π^- flux present in the beam resulted from $K_S^0 \to \pi^+\pi^-$ decays in this same neutral channel. The antiproton and pion fluxes collected in the high acceptance secondary beam transport were identified by two 21 meter long differential Cerenkov counters just upstream of the spectrometer. The first counter was set to detect antiprotons and the second counter was set to detect π^-. No K^- component was present in the beam because of its tertiary nature. The electron contamination resulting from photon conversions in the neutral channel was eliminate by placing a 2.5 cm lead absorber in the beam 180 m upstream of the spectrometer. Due to the large momentum bite of the beam ($\frac{\Delta p}{p} \sim 10\%$), it was necessary to measure the momentum of the beam particles on an event by event basis with a tagging system consisting of bending magnets and three stations of wire chambers and scintillator hodoscopes. This system also measured the position and incident angles of the beam particles at the spectrometer target. The beam tagging system operated routinely at 10^7 particles/second, allowed separation of $\bar{p}$ and π^- with less than 1% contamination of the antiproton flux, and measured beam momentum to approximately 1% accuracy.

The front section of the spectrometer consisted of a 1 or 1.5 absorption length W, Cu or Be target followed by 149 cm of Cu absorber to range out the hadrons. Imbedded in the Cu absorber was a proportional chamber whose purpose was the improvement of the measurement of the dimuon opening angle. Following the absorber were 9 drift chamber planes and a large (91 cm x 183 cm) aperture magnet which provided 27.7 kG meters of magnetic field. The rear section of the spectrometer contained 12 large drift chamber planes followed by a 230 element x,y scintillator hodoscope. The last element of the spectrometer was a muon detector which consisted of three large scintillator hodoscope planes imbedded in steel and concrete. The total thickness of copper hadron absorber and the muon detector imposed a 6 GeV momentum cutoff for muons.

The dimuon trigger consisted of a fast logic section followed by a higher level trigger processor.[2] The major requirement of the fast trigger was a triple coincidence among appropriate elements of the three muon hodoscope planes in at least two different quadrants of the detector. If the fast trigger conditions were met, the trigger processor searched for tracks in regions of the drift chambers indicated by the triple coincidences. Momentum and angles were determined for every track found by the trigger processor and the invariant masses of all pairs of tracks were calculated. Events with at least one pair with mass greater than 2 GeV/c^2 were recorded.

The spectrometer acceptance as a function of dimuon mass, x_F and p_T was calculated by a Monte Carlo program which included geometry, multiple scattering and trigger effects. The acceptances used in the cross sections presented in this paper assume a decay angular distribution of $1 + \cos^2 \theta^*$ where θ^* is the angle of one of the decay muons with respect to the beam direction in the dimuon rest frame (Gottfried-Jackson frame). The azimuthal angle of the muon in this same frame is distributed isotropically. These distributions are predictions of the Drell-Yan model discussed below and are consistent with the preliminary angular distributions observed in this experiment.

Unless indicated otherwise, errors quoted in this paper are statistical only. The present estimate of overall systematic uncertainties in the absolute cross sections is $\pm$ 20% arising from several sources (reinteractions in the thick target, trigger efficiencies, Fermi motion corrections, track finding efficiencies, beam normalization). The studies of these systematics are underway and the systematic error is expected to decrease substantially.

The mass spectra of the antiproton and pi minus induced dimuon events shown in Figs. 2a and b both exhibit clear J/ψ peaks. The mass resolution at the J/ψ is dominated by the uncertainty in the opening angle of the μ pair due to multiple scattering of muons in the copper absorber and the target. The analysis of the J/ψ production is presented elsewhere.[3] In this paper we report on the high mass ($M > 4$ GeV/c^2) dimuon events from approximately 85% of the total data (1015 π^- induced and 347 $\bar{p}$ induced dimuons). Only data from the tungsten target are reported. We have used an A dependence, $\sigma(Z,A) = \sigma_o(Z,A)\, A^{1.0}$, which is consistent with the Drell-Yan model and the experiments of Ref. 4, to calculate the per nucleon cross section. $\sigma_o(Z,A)$ in this formula is the 'average' cross section per nucleon for a nucleus of Z protons and A-Z neutrons.

The differential cross sections as a function of p_T and x_F for this sample of events are shown in Figs. 3 and 4. The shape and magnitude of the p_T distributions (integrated over the $x_F > 0$ region) are almost identical for π^- and $\bar{p}$ production. The ratio of the integrated cross sections

$\frac{\sigma(\bar{p}N \to \mu^+\mu^- + X)}{\sigma(\pi^-N \to \mu^+\mu^- + X)}$ above 4 GeV/c^2 and for $x_F > 0$ extracted from this data was found to be 0.93 ± 0.15 (systematic error is included). Both the pion and the antiproton p_T distributions fit well the empirical form $\frac{1}{p_T}\frac{d\sigma}{dp_T} = A\left(1 + \frac{p_T^2}{(3.1)^2}\right)^{\alpha}$ with $A_\pi = (1.89 \pm 0.08)\ 10^{-34}\ \mathrm{cm}^2\ \mathrm{GeV}^{-2}\ c^2$/nucleon, $\alpha_\pi = -9.3 \pm 0.4$, and $A_{\bar{p}} = (1.94 \pm 0.10)\ 10^{-34}\ \mathrm{cm}^2\ \mathrm{GeV}^{-2}\ c^2$/nucleon, $\alpha_{\bar{p}} = -10.2 \pm 0.6$. The average p_T^2 from these fits for all our antiproton and pion data is $\langle p_T^2\rangle_{\bar{p}} = 1.17 \pm 0.09$ GeV^2/c^2 and $\langle p_T^2\rangle_\pi = 1.32 \pm 0.07$. In contrast to the similarity of the p_T distributions, the x_F dependencies for the pion and antiproton cross sections are markedly different. The x_F cross section for the pion induced dimuon system is shifted forward of $x_F = 0$ and is much larger than the $\bar{p}$ cross sections in the high x_F region. One interpretation of this data is that the quark whose interaction leads to the production of a high mass dimuon is on the average more energetic in the case of a pion than in the case of an antiproton. Similar effects are seen in our J/ψ production data[3]. These x_F distributions fit a simple gaussian form $\frac{d\sigma}{dx_F} = A\, e^{-\frac{(x_F - b)^2}{2\sigma^2}}$ with $A_\pi = (1.6 \pm 0.1)\ 10^{-34}\ \mathrm{cm}^2$/nucleon, $b_\pi = 0.21 \pm 0.04$, $\sigma_\pi = 0.34 \pm 0.03$, and $A_{\bar{p}} = (2.7 \pm 0.2)\ 10^{-34}$ cm^2/nucleon, $b_{\bar{p}} = 0.0$ (fixed), $\sigma_{\bar{p}} = 0.27 \pm 0.02$.

We have compared our data to the predictions of the Drell-Yan model[5] in which an antiquark annihilates with a quark to produce a massive muon pair via a virtual photon. This model predicts a double differential cross section given by

$$\frac{d^2\sigma}{dx_F dM} = \frac{8\pi\alpha^2}{9M^3} \frac{\tau}{\sqrt{x_F^2 + 4\tau}} \sum_i e_i^2 \left[q_i^{h_1}(x_1)\, \bar{q}_i^{h_2}(x_2) + (1 \leftrightarrow 2) \right] \qquad (1)$$

where M is the dimuon mass and x_F is the Feynman scaling variable ($x_F = 2p^*_{||}/\sqrt{s}$) of the dimuon in the beam-target center of mass. x_1 and x_2 are the fractions of the beam and target hadron momentum carried by the interacting quarks with structure functions $q_i^{h_1}$ and $q_i^{h_2}$, respectively. In addition, the usual relations $\tau = M^2/s = x_1 x_2$ and $x_F = x_1 - x_2$ hold.

The $\bar{p}$N reaction is particularly valuable in ascertaining the validity of the Drell-Yan formula because the valence quark structure functions of the nucleon are measured independently in deep inelastic scattering experiments. In the case of the pion induced dimuons, Eq. (1) must be assumed to extract the pion structure functions. We have used the CDHS[6] nucleon structure functions at $Q^2 = 20\ \mathrm{GeV}^2/c^2$ and Eq. (1) to calculate the dimuon cross sections to compare with our $\bar{p}$ data. The 150 GeV π^- structure functions extracted by NA3[7] were required in addition to calculate the π^- cross sections for comparison with our π^- data. Figure 4 shows the predictions of the model as a function of x_F for antiprotons and pions. Figure 5a gives the prediction as a function of $\sqrt{\tau}$ for antiprotons. Figure 5b shows the scaling property of the pion data $M^3 \frac{d\sigma}{dM}$ for a range of pion energies. The shape of the spectra are well predicted but the overall level is low in both reactions. The preliminary values of the factors which are required to renormalize the prediction of the model to both sets of data is $K_{\bar{p}} = 2.25 \pm 0.45$ and $K_{\pi^-} = 2.5 \pm 0.5$ (current estimates of systematic errors are included).

The p_T dependence of the antiproton and pi minus data in Fig. 3 has been compared to a model of Altarelli, Parisi, and Petronzio[8] which provides a prescription to convolute the components of the dimuon p_T resulting from the intrinsic k_T (or non-perturbative) of the quark constituents with the component of the p_T due to the first order QCD quark-antiquark annihilation and gluon Compton scattering processes. The intrinsic k_T distribution is assumed to be gaussian in this model. An average k_T^2 of 0.88 GeV^2/c^2 has been observed in proton-nucleon interactions[9] when that data is analyzed with this model. We have used this average $\langle k_T^2 \rangle$, the previously mentioned quark structure functions and counting rule gluon structure functions $\{G_\mu(x) = 3.06\ (1-x)^5;\ G_\pi(x) = 2.0\ (1-x)^3\}$ to calculate the Altarelli prediction for the p_T distributions shown in Fig. 3. We find that $\langle k_T^2 \rangle = 0.88\ GeV^2/c^2$ is consistent with the data even though in the case of the antiproton or pion reaction, valence-valence interactions rather than sea-valence interactions dominate the cross sections. In addition in our higher statistics pion data the high p_T tail is consistent with the quark-antiquark annihilation into a high p_T virtual photon and a gluon. In Fig. 6 we show the average $\langle p_T^2 \rangle$ at $\tau = 0.28$ as a function of s for the composite of experimental data[10] on pion induced dimuons. The observed linear behavior is in agreement with the expected QCD behavior.

In conclusion, the preliminary analysis of our antiproton and pion induced dimuon events has yielded cross sections which are consistent with the Drell-Yan predictions if K factors of

2.25 ± 0.45 and 2.5 ± 0.5 for $\bar{p}$ and π^- respectively are applied. The x_F distributions are quite different reflecting the differences in the structure functions of the two beam particles. The p_T spectra of the $\bar{p}$ and π^- reactions are remarkably similar considering the different quark structure of pions and antiprotons and are consistent with an intrinsic $\langle k_T^2 \rangle = 0.88\ \mathrm{GeV}^2/c^2$.

We wish to thank the personnel of the Fermilab Proton Department and the Fermilab Physics Section for invaluable aid over the course of this experiment. We would also like to thank the U.S. Department of Energy, the National Science Foundation-International Programs and -High Energy Physics Divisions, the Natural Sciences and Engineering Research Council of Canada, Quebec Department of Education, and the Hellenic Science and Technology Agency for their support.

REFERENCES

1. B. Cox, Fermilab Report 79/1, 0090.01, January (1979).

2. P. Kostarakis, *et al.*, Topical Conference on the Application of Microprocessors to High Energy Physics Experiments, CERN, 4 May 1981.

3. J/ψ Resonance Production in 125 GeV/c $\bar{p}N$ and $\pi^{-}N$ Interactions, submitted to the XXI International High Energy Physics Conference, Paris, France (1982).

4. S. Falciano, *et al.*, NA10 Collaboration, Phys. Letters 104B, 416 (1981); J. Badier, *et al.*, NA3 Collaboration, Phys. Letters 104B, 335 (1981).

5. S.D. Drell and T.-M. Yan, Phys. Rev. Letters 25, 316 (1970).

6. J.G.H. deGroot, *et al.*, CDHS Collaboration, Phys. Letters 82B, 456 (1979).

7. D. Decamp, NA3 Collaboration, Proceeding of the XX International Conference on High Energy Physics, Madison, 149 (1980).

8. G. Altarelli, *et al.*, Phys. Letters 76B, 356 (1978).

9. A.S. Ito, *et al.*, Phys. Rev. D23, 604 (1981).

10. J. Bardeen, *et al.*, NA3 Collaboration, CERN-EP/80-150, (1980); K.J. Anderson, *et al.*, CIP Collaboration, Phys. Rev. Letters 42, 944 (1979); M.J. Corden, *et al.*, Omega Collaboration, Phys. Letters 96B, 417 (1980).

FIGURE CAPTIONS

Fig. 1 The E-537 Spectrometer.

Fig. 2a Mass distribution (corrected for acceptance) for $\bar{p}$-induced dimuon events.

Fig. 2b Mass distribution (corrected for acceptance) for π^--induced dimuon events.

Fig. 3 Differential cross sections $\frac{1}{p_T}\frac{d\sigma}{dp_T}$ for $x_F > 0$ and $M > 4$ GeV/c^2 for the antiproton and pi minus reactions. The solid curves are the predictions of the Altarelli et al. first order QCD calculations.

Fig. 4 Differential cross sections $\frac{d\sigma}{dx_F}$ for $M > 4$ GeV/c^2 dimuon events from antiproton and pi minus reactions. The curves are the predictions of the Drell-Yan model using the CDHS and NA3 structure functions for the nucleon and the pion respectively and the K factors quoted in the text.

Fig. 5a The scaling cross section $M^3 \frac{d\sigma}{dM}$ ($x_F > 0$) for 125 GeV/c antiproton induced dimuons. Also shown are the 150 GeV/c NA3 data points. The curve is the prediction of the Drell-Yan model using CDHS structure functions and a K factor of 2.3.

Fig. 5b The scaling cross section $M^3 \frac{d\sigma}{dM}$ ($x_F > 0$) for the 125 GeV/c pi minus induced dimuons. Other pion data taken at different energies are shown to demonstrate the energy scaling predicted by the simple Drell-Yan model.

Fig. 6 The $<p_T^2>$ of pion induced dimuons for several experiments as a function of s. The curve is a straight line drawn to demonstrate the observed linear behavior of the data. This linear increase with s is predicted by QCD.

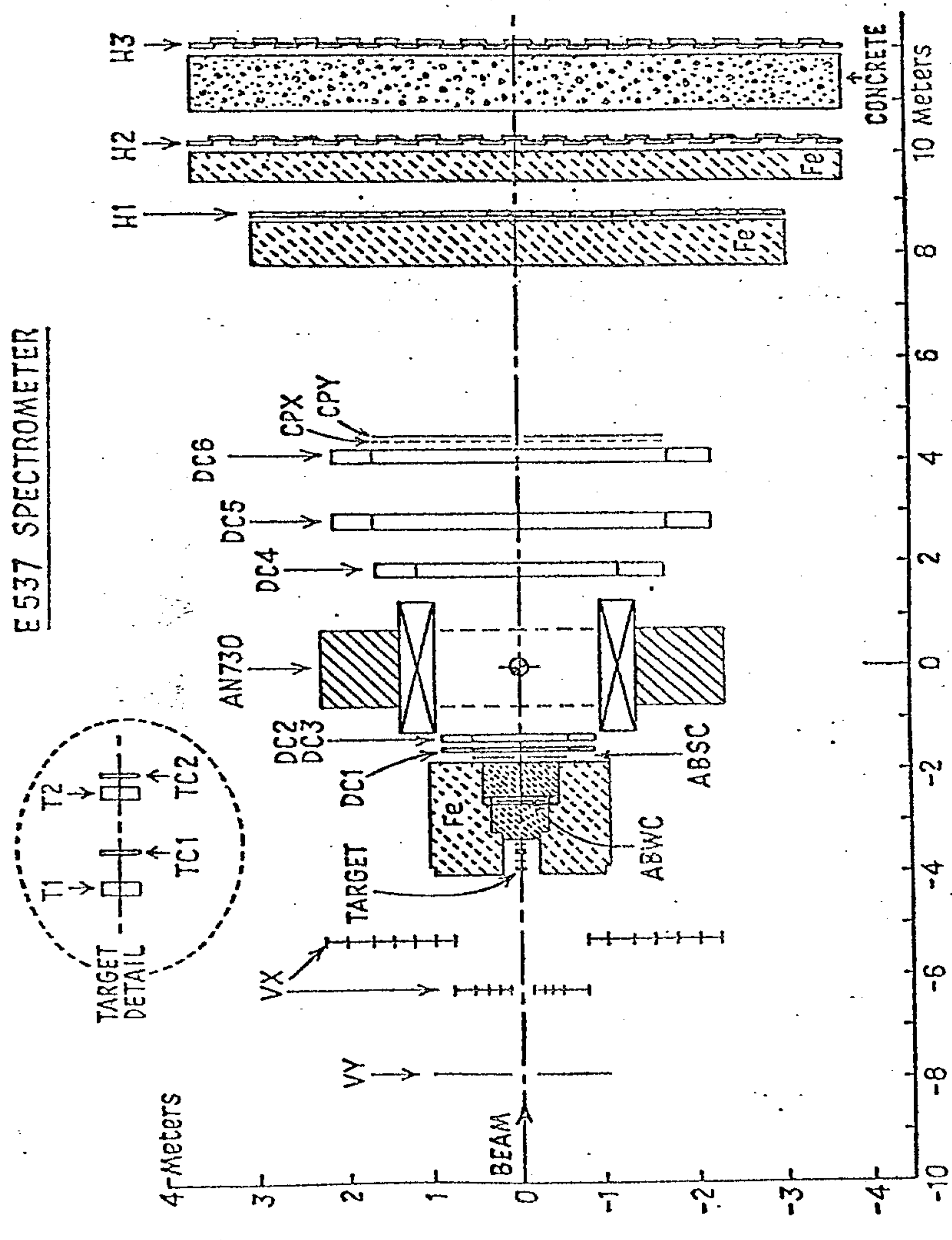

E 537 SPECTROMETER
TARGET DETAIL
T1
T2
TC1
TC2
VY
VX
TARGET
Fe
DC1
DC2
DC3
ABWC
ABSC
AN730
DC4
DC5
DC6
CPX
CPY
H1
H2
H3
Fe
Fe
CONCRETE
BEAM
Meters
10 Meters
4
3
2
1
0
-1
-2
-3
-4
-10
-8
-6
-4
-2
0
2
4
6
8

FIG. 1

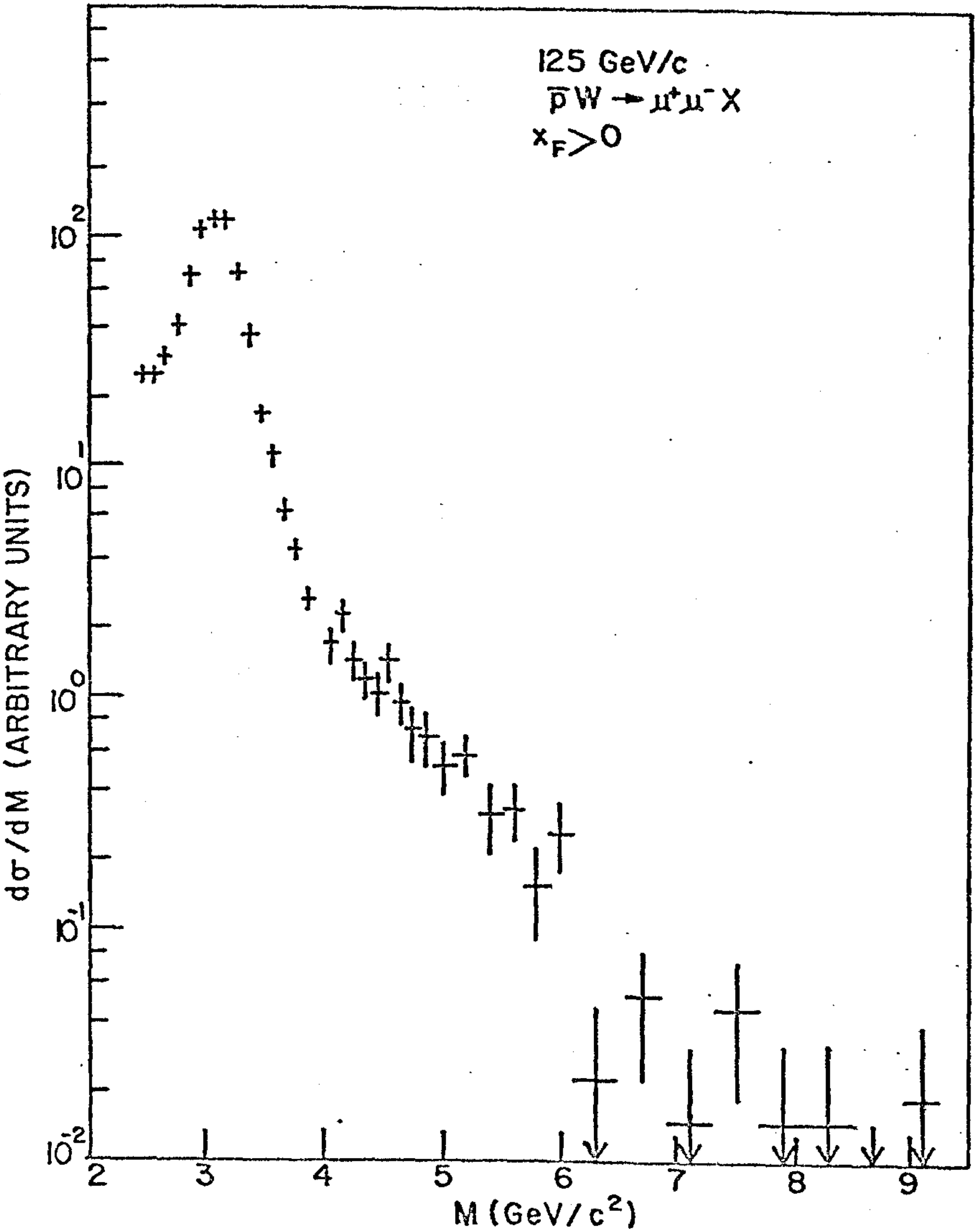

125 GeV/c
$\bar{p}W \to \mu^+\mu^- X$
$x_F > 0$
$d\sigma/dM$ (ARBITRARY UNITS)
10^2
10^1
10^0
10^{-1}
10^{-2}
2
3
4
5
6
7
8
9
M (GeV/c^2)

FIG. 2a

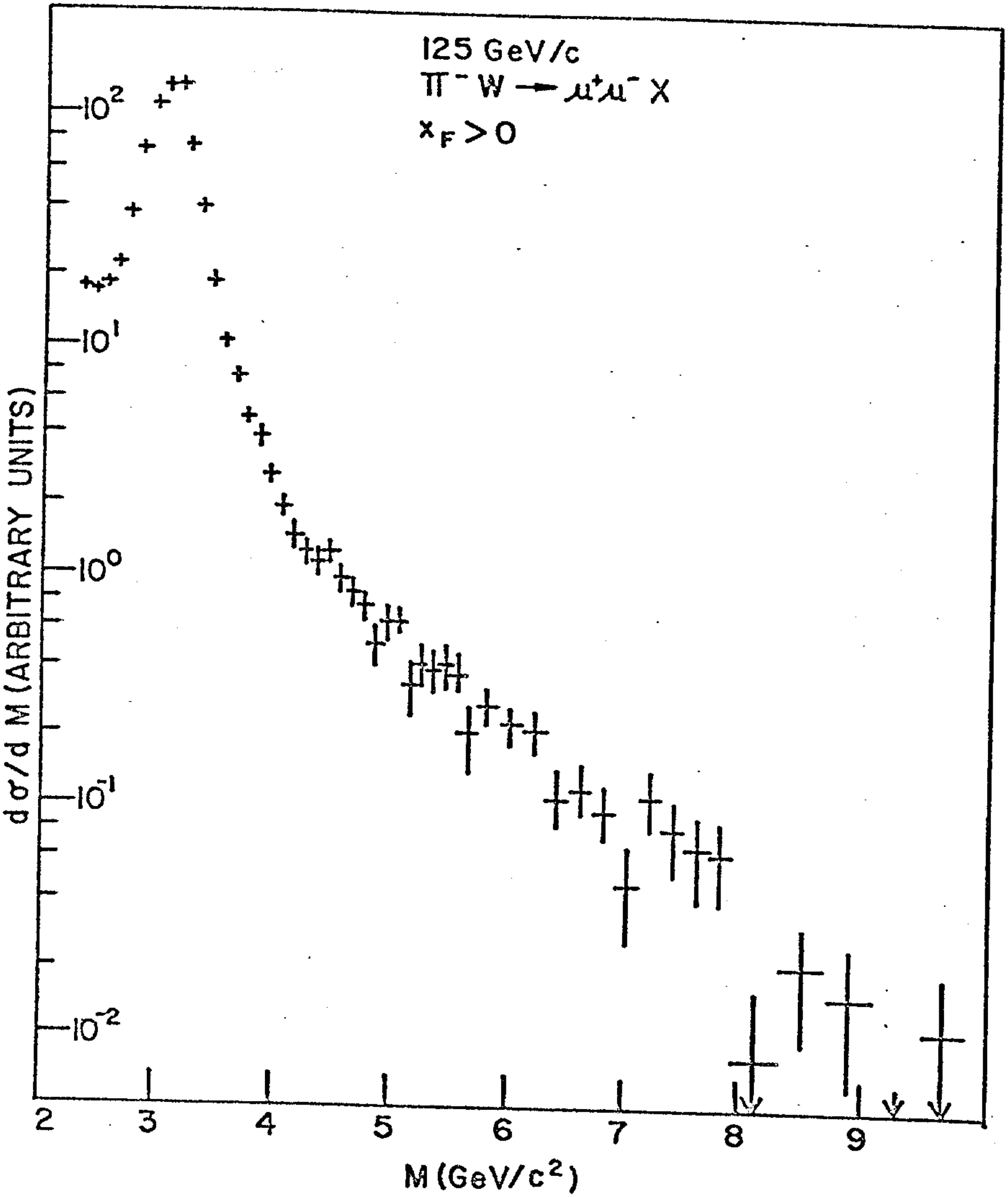
125 GeV/c
$\pi^- W \to \mu^+\mu^- X$
$x_F > 0$
$d\sigma/dM$ (ARBITRARY UNITS)
10^2
10^1
10^0
10^{-1}
10^{-2}
2
3
4
5
6
7
8
9
M (GeV/c^2)

FIG. 2b

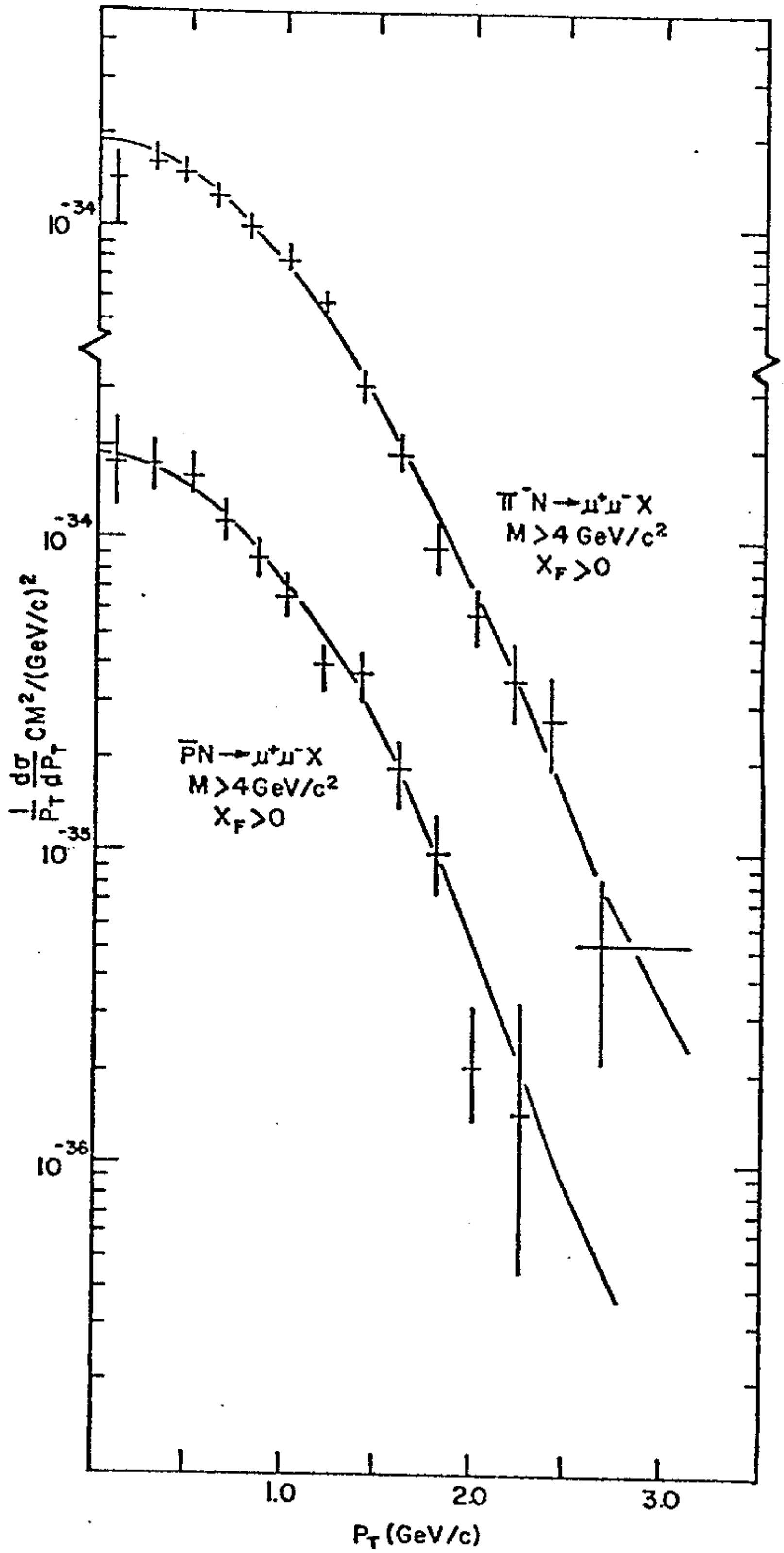

10^{-34}
10^{-34}
10^{-35}
10^{-36}
$\frac{1}{P_T}\frac{d\sigma}{dP_T}$ CM^2/(GeV/c)^2
$\pi^- N \to \mu^+\mu^- X$
$M > 4$ GeV/c^2
$X_F > 0$
$\bar{P}N \to \mu^+\mu^- X$
$M > 4$ GeV/c^2
$X_F > 0$
1.0
2.0
3.0
P_T (GeV/c)

FIG. 3

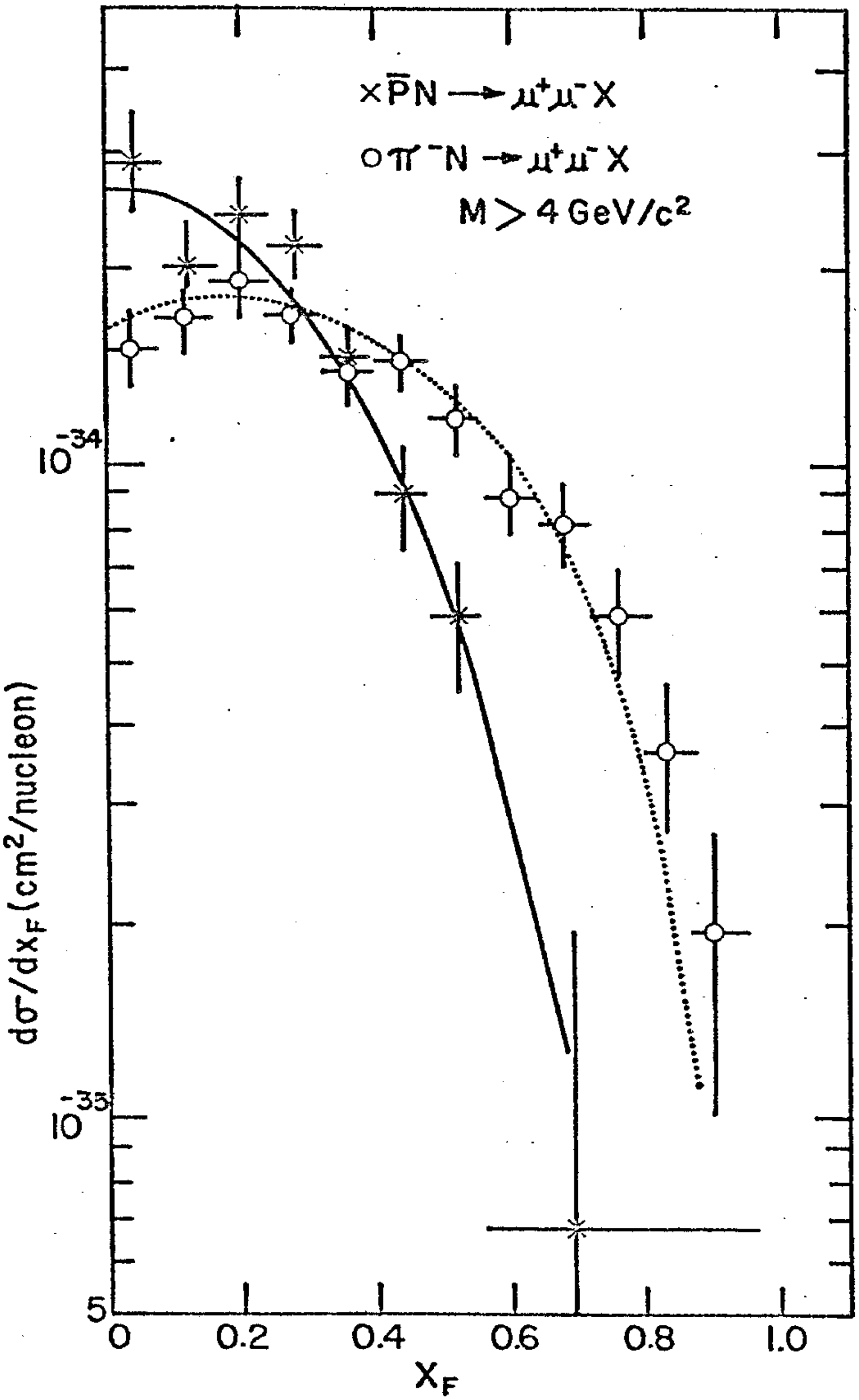

× $\bar{P}N \rightarrow \mu^+\mu^- X$
○ $\pi^- N \rightarrow \mu^+\mu^- X$
$M > 4\ GeV/c^2$
10^{-34}
10^{-35}
5
$d\sigma/dx_F\ (cm^2/nucleon)$
0
0.2
0.4
0.6
0.8
1.0
X_F

FIG. 4

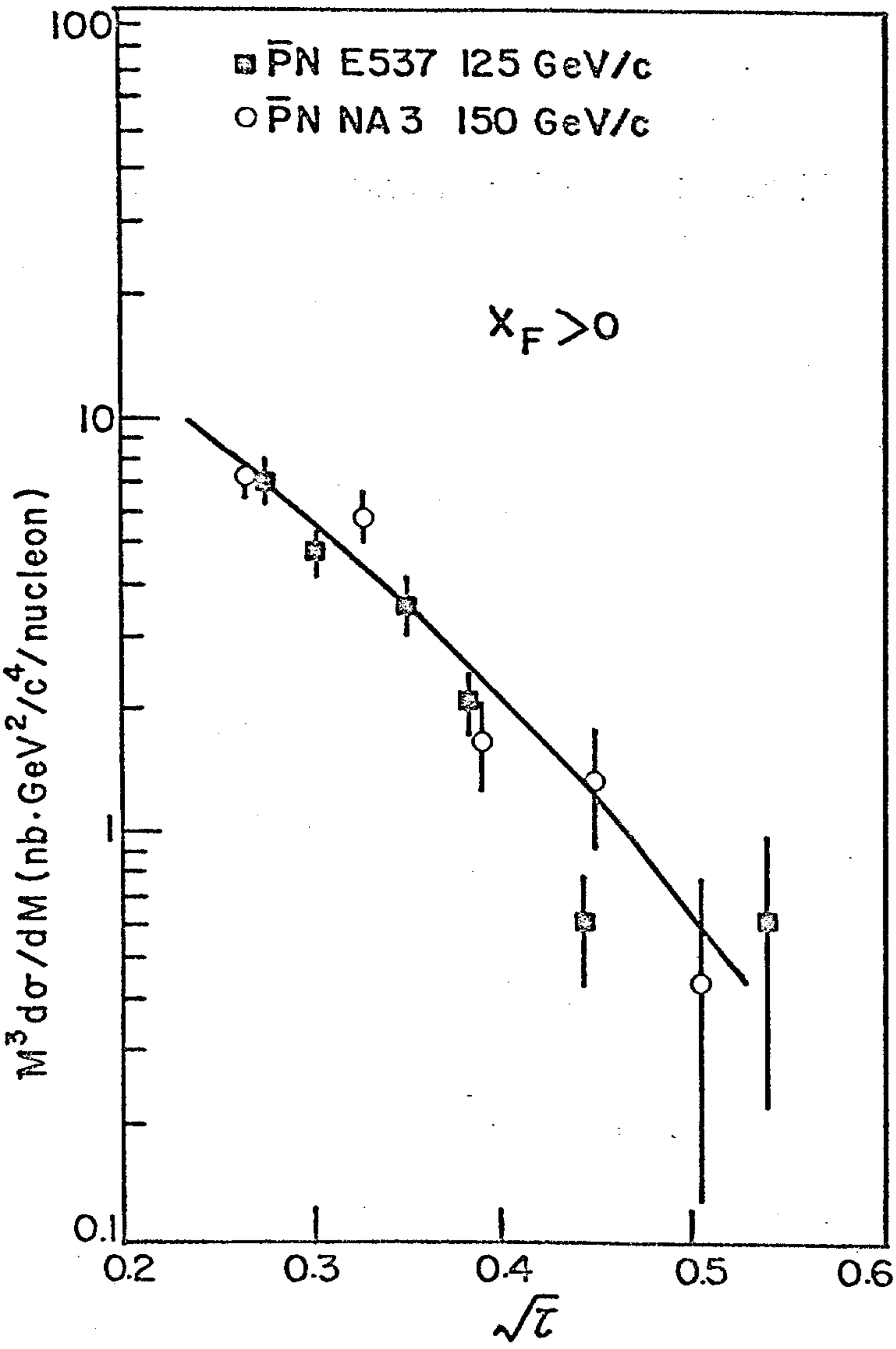

▪ $\bar{P}N$ E537 125 GeV/c
○ $\bar{P}N$ NA3 150 GeV/c
$X_F > 0$
$M^3 d\sigma/dM$ (nb·GeV^2/c^4/nucleon)
100
10
1
0.1
0.2
0.3
0.4
0.5
0.6
$\sqrt{\tau}$

FIG. 5a

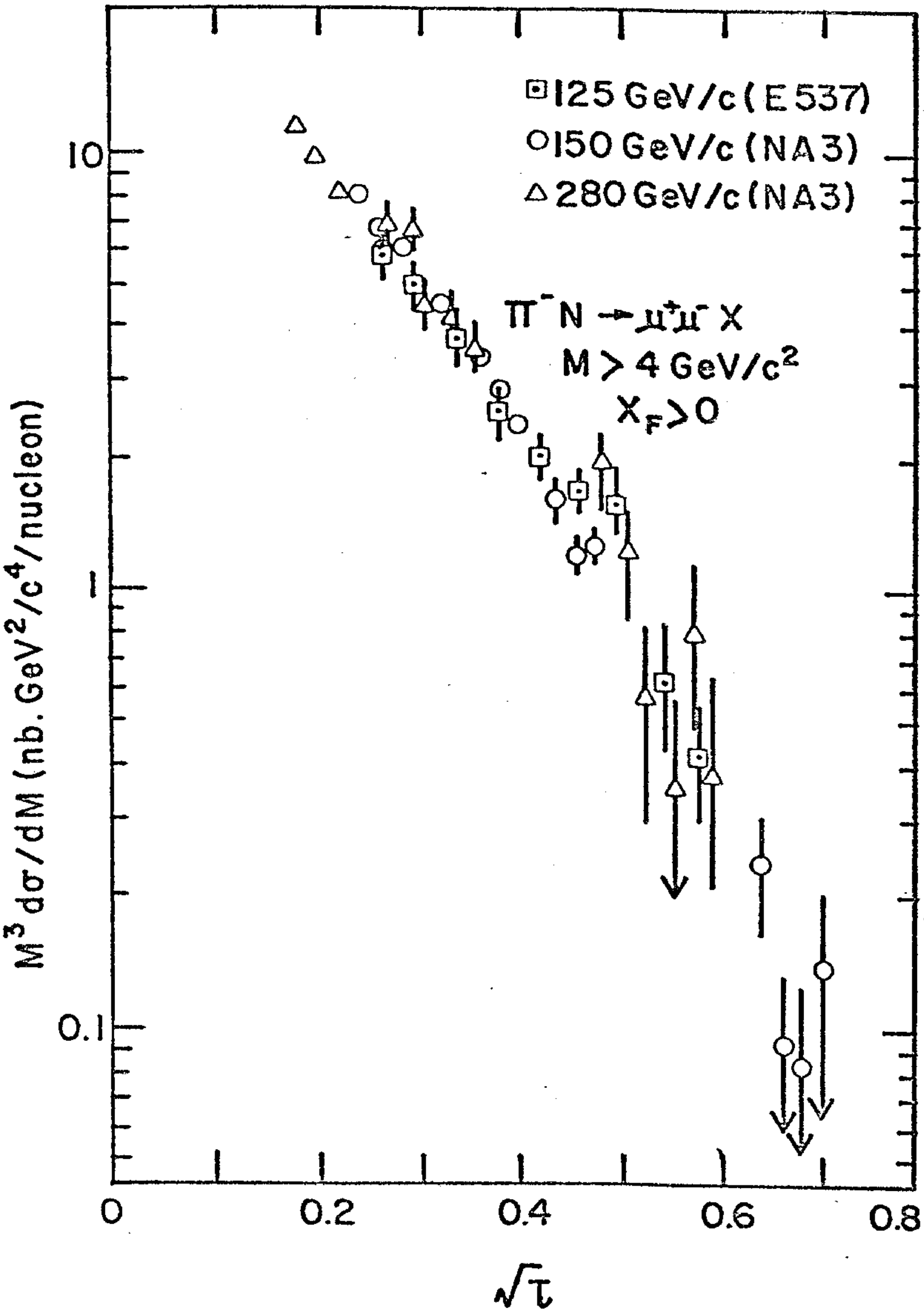

125 GeV/c (E 537)
150 GeV/c (NA3)
280 GeV/c (NA3)
π⁻N → μ⁺μ⁻ X
M > 4 GeV/c²
X_F > 0
M³ dσ/dM (nb. GeV²/c⁴/nucleon)
10
1
0.1
0
0.2
0.4
0.6
0.8
√τ

FIG. 5b

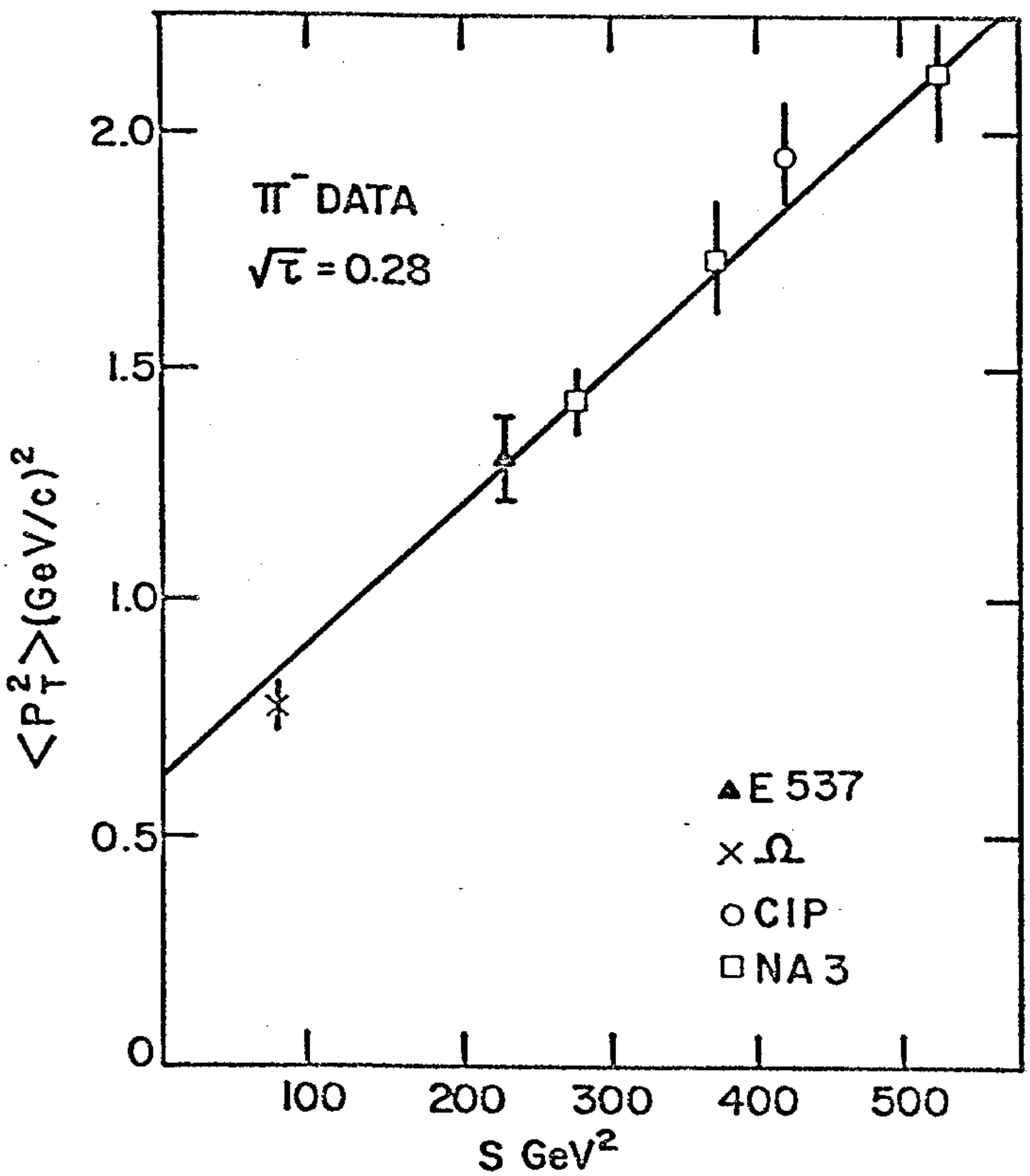

π⁻ DATA
√τ = 0.28
E 537
Ω
CIP
NA 3
2.0
1.5
1.0
0.5
0
100
200
300
400
500
S GeV²
<P²T>(GeV/c)²

FIG. 6